

Low-energy excess of vibrational states in v-SiO₂: the role of transverse dynamics

O. Pilla¹, A. Fontana¹, J. R. Gonçalves^{1,2}, G. Viliani¹, L. Angelani³

¹*INFN and Dipartimento di Fisica, Università di Trento, 38050 Povo, Trento, Italy*

²*Departamento de Física, Universidade Federal do Ceará,*

C.P. 6030, Campus do Pici, 60455-760 Fortaleza, Ceará, Brazil

³*INFN, SMC-INFN, and Dipartimento di Fisica,*

Università di Roma La Sapienza, Piazzale Aldo Moro 2, 00185 Roma, Italy

(Dated: March 22, 2022)

The study of the effects of the density variations on the vibrational dynamics in vitreous silica is presented. A detailed analysis of the dynamical structure factor, as well as of the current spectra, allows the identification of a flattened transverse branch which is highly sensitive to the density variations. The experimental variations on the intensity and position of the Boson Peak (BP) in v-SiO₂ as a function of density are reproduced and interpreted as being due to the shift and disappearance of the latter band. The BP itself is found to correspond to the lower energy tail of the excess states due to the piling up of vibrational modes at energies corresponding to the flattening of the transverse branch.

PACS numbers: 61.43.Bn, 61.43.Fs, 63.50.+x

I. INTRODUCTION

In this paper we address one of the still open questions in physics of glasses: the origin of the excess of vibrational states in the low energy region with respect to the usual Debye density of states.^{1,2} This excess, characteristic of every glassy system, gives rise to the presence, in the region below a few meV, of a more or less pronounced peak, observed both in Inelastic X-ray-Scattering (IXS), Inelastic Neutron-Scattering (INS), and Raman spectra. This peak is universally referred to as Boson Peak (BP). Despite its universality, different interpretations and hypotheses have up to now been proposed both on its origin and on the nature of the excess vibrational states. On the basis of experimental observations and computer simulations, these modes have been catalogued as spatially localized,^{1,3} spatially delocalized and propagating,^{4,5,6} spatially delocalized but diffusive in character.⁷ Theoretical investigations, on the other hand, have interpreted the BP in glasses as arising from the lowest-energy van Hove singularity of the corresponding crystal;^{8,9} or as the precursor of a dynamical instability expected in a disordered structure;¹⁰ or as arising from the high frequency dynamics of a model glass within a mode-coupling-like description of Götze¹¹ and of Theenhaus.¹²

Particularly in the case of v-SiO₂ at normal density the most widely accepted explanation is that the BP originates from the piling up of modes near the first van-Hove singularity of the transverse acoustic vibrational branch.^{8,9} These modes should mainly involve relative rotations of almost rigid SiO₄ tetrahedra as early pointed out by Buchenau and coworkers.¹ In addition to the ambient pressure data, a much useful information is available in the case of v-SiO₂ for higher densities, obtained both from *in-situ* measurements and from permanently densified samples. In general, densification results in a shift of the BP towards higher energies and in a simultaneous decrease of its intensity.^{13,14,15,16}

In addition to the experimental data, the BP behavior with density has been successfully reproduced by a series of simulations.^{17,18,19} Recently, very accurate INS measurements on densified vitreous silica (d-SiO₂) have confirmed these effects.^{20,21,22} In densified samples the BP lies at higher energies than in vitreous silica at normal density and has a rather weaker intensity. In densified samples the inelastic signal in the BP energy range shows a more marked dependence on the scattering wavevector Q as regard its intensity and peak position. We present here simulation results on v-SiO₂ at different densities which, when compared with the existing experimental data, can help in clarifying the origin and the nature of the excess modes as well as the intensity and shift effects on the BP as a function of density.

II. SIMULATION

The simulated system was a glass consisting of 680 SiO₂ molecules interacting through the modified BKS two-body interaction potential,^{23,24} with periodic boundary conditions. After a long thermalization at a density of 2.2 g cm⁻³ and at 5000 K the system was slowly cooled down to 300 K at constant volume. At this temperature, an energy minimization was performed to locate the equilibrium configuration at room pressure. The box size was then stepwise scaled by 1.5% amounts up to the final density of 4.0 g cm⁻³. Once reached this value, the density was decreased in the same way. At each step the energies of the individual realizations were minimized using geometrical methods to obtain the relative equilibrium configurations. This procedure mimics a real hydrostatic pressure experiment at room temperature as described in detail elsewhere.¹⁹ The pressure was estimated by using the virial theorem and compared to experimental data.^{14,25} After the density cycle the zero pressure realization had a density of about 2.8 g cm⁻³.

The dynamical properties of the two zero pressure configurations, and of the higher density ones, were computed in the harmonic approximation by diagonalizing the dynamical matrix. In particular, we have computed the density of states $g(E)$ and the longitudinal and transverse currents spectra ($C(Q, E)$) which, in the one-excitation approximation, are given by:

$$C_{\alpha\beta}^L(Q, E) = \frac{K_B T}{\sqrt{M_\alpha M_\beta}} \cdot \Sigma_p |\Sigma_n (\hat{Q} \cdot \bar{e}_p(n)) \exp(i \bar{Q} \cdot \bar{R}_n)|^2 \cdot \delta(E - E_p)$$

$$C_{\alpha\beta}^T(Q, E) = \frac{K_B T}{\sqrt{M_\alpha M_\beta}} \cdot \Sigma_p |\Sigma_n (\hat{Q} \times \bar{e}_p(n)) \exp(i \bar{Q} \cdot \bar{R}_n)|^2 \cdot \delta(E - E_p) \quad (1)$$

where α, β indicate Si and O, and $\hat{Q} = \bar{Q}/|Q|$.

The current spectra in transverse polarization are, contrary to the longitudinal currents, not experimentally measurable, and thus they are not directly observable by means of inelastic scattering experiments at least in the low- Q and low- E ranges. They are nonetheless very useful in understanding the details of the vibrational dynamics, as will be explained in the following section.

III. DISCUSSION

A. Current Spectra

Usually the dynamical data obtained via simulation are reported showing the dynamical structure factor, $S(Q, E)$. This is mainly because this procedure has the advantage of being directly comparable to the experimental spectra obtained, for instance, from standard INS and IXS measurements. On the other hand, the current spectra, defined as $C(Q, E) = E^2 S(Q, E)/Q^2$, are much more useful when one is interested in characterizing the vibrational spectra. In fact, each current spectrum, taken at a fixed E and $C(Q, E)$, gives the Q -characterization of the individual vibration with energy E , being the current strictly related (in harmonic approximation) to the power spectrum of the Fourier transform of the corresponding eigenvector. The computed current spectra, both for longitudinal and transverse dynamics, are shown in Fig. 1 (upper and lower panel, respectively) as a contour map plot for v-SiO₂ at $\rho = 2.2, 2.8, 4.0 \text{ g cm}^{-3}$. The most evident feature is that in the longitudinal currents a periodicity is present, even if much less evident than in a crystal. The same feature is present in the transverse ones, but with a longer quasi period which extends beyond the limit of the figure.

As discussed elsewhere,^{19,26} this difference is due to the fact that the longitudinal dynamics is affected by the average height of the SiO₄ tetrahedron, which is the main structural unit of v-SiO₂, while the transverse vibrations are sensible to the average height of SiO₄ tetrahedron decorated with oxygen atoms. In the low- Q longitudinal

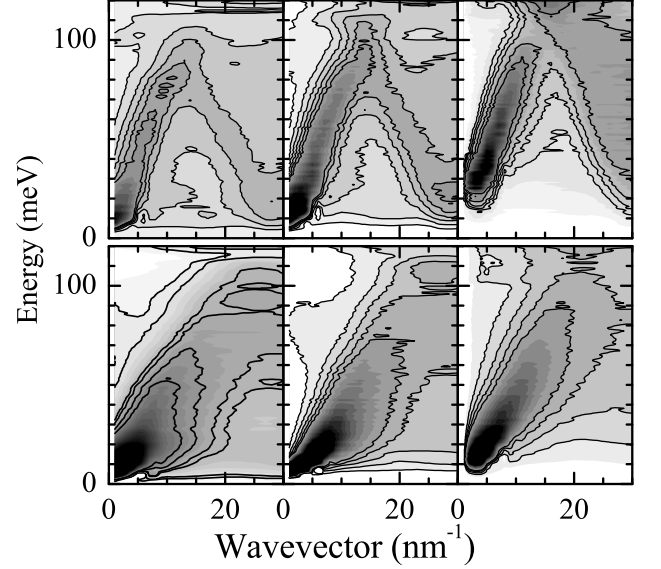


FIG. 1: Computed currents relative to neutron scattering grey scale maps for v-SiO₂ at three different densities (from left to right): $\rho = 2.2 \text{ g cm}^{-3}$ ($P = 0 \text{ GPa}$), $\rho = 2.8 \text{ g cm}^{-3}$ ($P = 0 \text{ GPa}$ densified); $\rho = 4.0 \text{ g cm}^{-3}$ ($P = 35 \text{ GPa}$). Upper panels: longitudinal currents; lower: transverse. The current spectra have been divided by Q^2 for visualization purposes.

spectrum, in addition to the quasi-periodic pattern, two well observable features are present in the two lowest-density samples, which consist of protruding peninsulae, nearly parallel to the Q axis, centered at about 20 and 100 meV. These features have been interpreted²⁶ as a trace of the vibrational dynamics of the cristobalite structure (the crystalline counterpart of v-SiO₂), which shows in that energy range flat dispersion bands. It should be noted that the plots of Fig. 1 are shown as a function of the modulus of the wavevector, which is a relevant quantity in glasses, thus losing every information on the Q -direction. If this convention were used also in representing the dispersion curves of a crystal, different Q -directions in the Brillouin zone would superimpose giving qualitatively the same effect as in Fig. 1. In the Q - E range between 5 and 15 nm⁻¹ and 10 to 25 meV (where the flat band is observed in the longitudinal currents) a much more evident flattening is present in the transverse currents. This coincidence has suggested the interpretation that the flattened band in the longitudinal currents arises from a spilling of transverse dynamics into the longitudinal one, due to disorder.^{19,25,26,27}

The maxima of the longitudinal and of the transverse currents in the constant Q cuts, are reported in Fig. 2 for three different densities.

In the starting configuration, $\rho = 2.2 \text{ g cm}^{-3}$, open

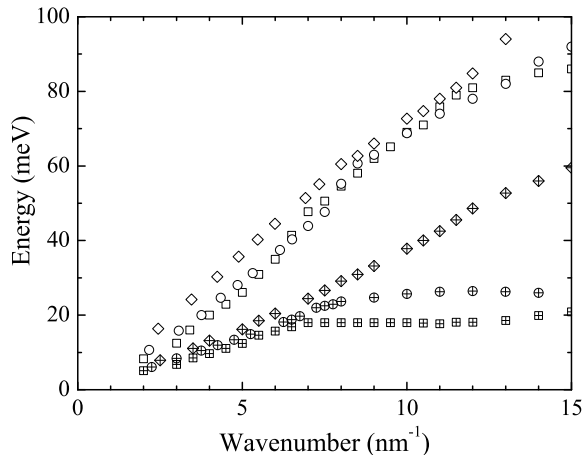


FIG. 2: Main maxima of the longitudinal (open symbols) and transverse (crossed symbols) current spectra, for three different densities. Squares: $\rho = 2.2 \text{ g cm}^{-3}$ ($P = 0 \text{ GPa}$); diamonds: $\rho = 4.0 \text{ g cm}^{-3}$; circles $\rho = 2.8 \text{ g cm}^{-3}$ ($P = 0 \text{ GPa}$ densified).

and crossed squares of Fig. 2, the main maxima relative to the longitudinal currents have a rather defined dispersive character up to very high energies (about 100 meV), while the transverse dispersion one flattens at small Q -values. The transverse maxima remain centered, within the uncertainty, at the same energy where a minor peak is observed also in the longitudinal current spectra, whose intensity is roughly 50 to 80% of the main feature.²⁵ By increasing the density up to 4.0 g cm^{-3} , the local structure of the glass, which at normal density consists of fourfold coordinated Si ions, is almost completely substituted by an octahedral one (typical of stishovite, the crystalline form of silica, stable at high densities). As a consequence, also the dynamical properties change and this can be seen in Fig. 2. Both longitudinal and transverse maxima follow a nearly linear dispersion law up to the highest energies and no flattening is observed.

B. Boson Peak

From our simulations we calculated also the density of states as a function of the density. The result are shown in Fig. 3 for selected densities. The low energy part of the total density of states shifts toward higher frequencies and decreases in intensity with increasing density. As a consequence, the BP strongly decreases in intensity and shifts at high energies¹⁹.

The reduction of the intensity of the BP with the density can be ascribed to two concurring effects. The first one is an overall reduction of excess states, induced by the pressure, and the second one is the shift towards

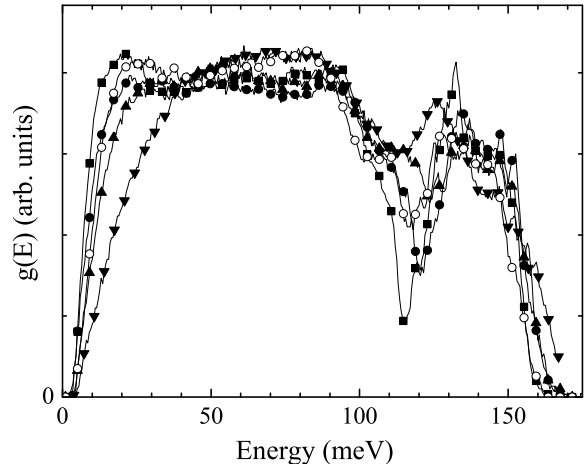


FIG. 3: Vibrational density of states of v-SiO₂ at different densities: full squares: $\rho = 2.2 \text{ g cm}^{-3}$; full circles: $\rho = 2.8 \text{ g cm}^{-3}$; up triangles: $\rho = 3.2 \text{ g cm}^{-3}$; down triangles: $\rho = 4.0 \text{ g cm}^{-3}$; open circles: compressed sample $\rho = 2.8 \text{ g cm}^{-3}$ (zero pressure after pressure cycle).

high energies of the excess which, being weighed by an $1/E^2$ factor, appears as having a lower intensity. Actually, both mechanisms are effective in v-SiO₂ as we will discuss later. In Fig. 4 we present the maxima of the transverse currents computed at several densities. In the $\rho = 2.2 \text{ g cm}^{-3}$ sample, after a linear increase a flattening of the maxima of the transverse currents is observed for q -values higher than 6 nm^{-1} , at about 15 meV. This plateau progressively shifts, and eventually disappears with increasing density. In the highest density sample it is no more observed and only a linear dispersion relationship is present. By decreasing the density the plateau is at least in part recovered, as shown in the upper panel of Fig. 4. It is worth noting that in the densified sample at $P = 0 \text{ GPa}$ ($\rho = 2.8 \text{ g cm}^{-3}$) the flattening is present, but it saturates at an energy of about 5 meV higher than in the starting realization, indicating an hysteretic behaviour.

The shift and the disappearance of the plateau help in interpreting the intensity and the energy effects on the BP. The excess of states shifts to higher energies and progressively disappears. The fact that these effects take place in an energy region, i.e. 15 meV, higher than the one where the Boson Peak is observed, about 4 meV, is only an apparent contradiction. As a matter of fact, the presence of the $1/E^2$ factor severely affects the spectral shape of the excess states by weighting only their low-energy tail. Indeed, the true excess of states should be observed only in the *difference* between the computed density of states and its Debye approximation.

The determination of the actual shape of the vibrational excess is not a simple task, since it implies the

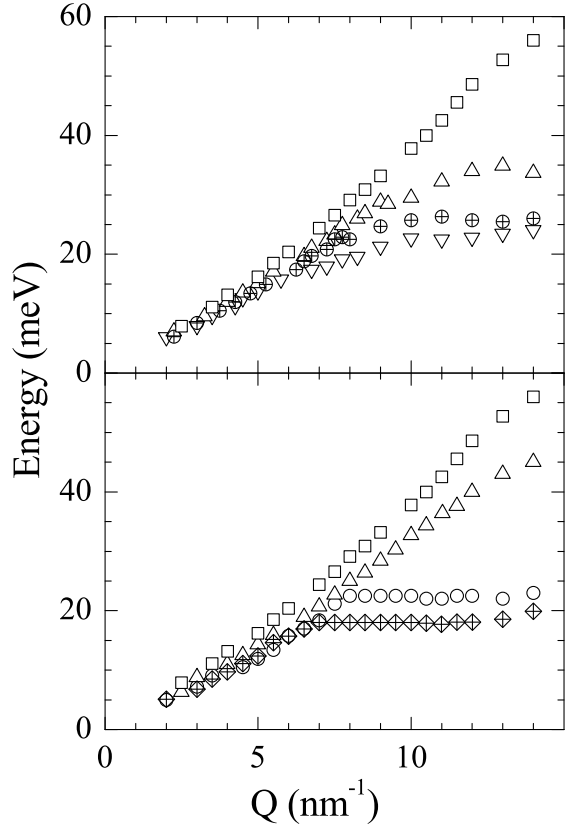


FIG. 4: Lower panel. Maximum of the transverse current spectra computed at different densities with increasing density. Diamonds, circles, triangles and squares correspond to $\rho = 2.2 \text{ g cm}^{-3}$, $\rho = 2.8 \text{ g cm}^{-3}$, $\rho = 3.2 \text{ g cm}^{-3}$, and $\rho = 4.0 \text{ g cm}^{-3}$, respectively. Upper panel. Maximum of the transverse current spectra measured at different densities with decreasing density. Down triangles, circles, up triangles and squares correspond to $\rho = 2.4 \text{ g cm}^{-3}$, $\rho = 2.8 \text{ g cm}^{-3}$, $\rho = 3.2 \text{ g cm}^{-3}$, and $\rho = 4.0 \text{ g cm}^{-3}$, respectively. The crossed symbols refer to the zero pressure realization, before and after the pressure cycle.

knowledge not only of the density of states, but also of the relative weight of the crystalline one, or at least its Debye approximation. The density of states can be obtained from inelastic neutron scattering data, and also, to a certain extent, from unpolarized Raman data. The Debye density of states can be independently estimated via Brillouin light scattering, while heat capacity experiments give the proper normalization factors.^{1,28}

The result of this procedure is shown in Fig. 5, where INS-deduced $g(E)$ is shown with the relative estimate of the Debye contribution. The excess of states (full line in the figure), obtained by subtracting the Debye from the DOS, is a very broad unstructured band centered at energies higher than 7 meV. By dividing this latter by

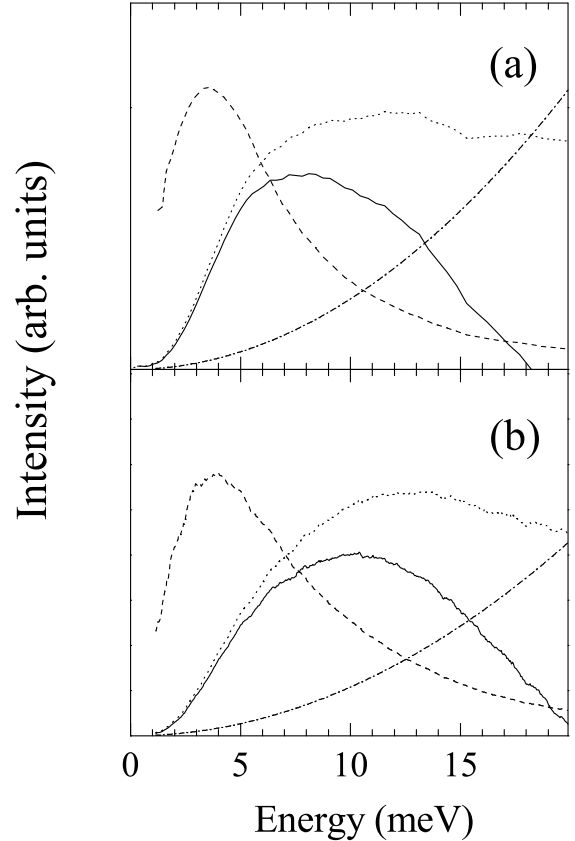


FIG. 5: (a) Dotted line: INS density of states of v-SiO₂; dash-dotted-line: Debye approximation; full line: vibrational excess, *i.e.* density of states minus Debye; dashed line: density of states divided by E^2 . (b) Same as (a) but for the unpolarized Raman spectrum of v-SiO₂. Here the full line represents the density of states weighted by the Raman coupling function.

E^2 its maximum shifts towards lower energies, less than 4 meV, as is shown in Fig. 5 dashed line. This latter peak corresponds to the Boson Peak observed both in INS and IXS measurements of the dynamical structure factor. Actually, the observed BP lies on the low energy tail of the true excess of states, since the contribution of the remaining high-energy vibrations is almost suppressed by the $1/E^2$ factor. A similar effect is observed also in the depolarized Raman spectra. Here one does not observe directly the density of states, but this quantity weighed by the Raman coupling function,²⁹ as shown in Fig. 5(b). A qualitatively similar behaviour is found even if the scattered intensity is somewhat deformed by the Raman coupling function $C(E)$.

The difference between the position of the maxima in the excess of states as found in simulations (about 17 meV as in Fig. 4) and in experiments (about 7 meV as in

Fig. 5), can derive from two main causes. From the computational point of view, the discrepancy may derive from the potential used. Moreover, the experimental density of states is obtained through some approximations, like f.i. the incoherent approximation and the estimate of the multiphonon contribution. Also, in the simulations the excess states could be overestimated due to unphysical quenching times currently used in Molecular Dynamics, as pointed out recently by Angell.³⁰ Finally, the behavior of the transverse current maxima with density shown in Fig. 4, not only accounts for the intensity decrease of the BP, but also explains the coherence effects of the BP measured with in INS and IXS as a function of the density. The BP in normal v-SiO₂ has a small coherence effect, i.e. it is rather insensitive to the exchanged wavevector.⁴ On the contrary, densified samples have a marked coherent behavior at least at small Q -values.²⁰ From Fig. 4 full circles, one sees that the coherence effects in the BP range, i.e. variation in position and/or intensity, are expected in the linear dispersing range in the case of the $\rho = 2.2 \text{ g cm}^{-3}$ sample, being the dispersion curve flat for wavevectors higher than 6 nm^{-1} . In the densified sample at zero pressure, $\rho = 2.8 \text{ g cm}^{-3}$, the linear region extends up to 9 nm^{-1} . In the latter sample it is indeed possible to study, using IXS, a more extended linear region and the direct observation of a Brillouin peak directly in the energy cuts is possible in spite of the resolution limitations. Hence, in the densified samples our simulations predict (i) in the low- Q , low- E range a dispersing region where a Brillouin peak is observed extending to wavevectors higher than than in normal silica measurements, (ii) the appearance of the BP (nearly Q insensitive) at wavevectors (and corresponding energies) higher than in v-SiO₂, (iii) a BP intensity weaker than that of the normal density sample. All these predictions

are confirmed by the experiments of Foret and coworkers,²⁰ while the energy shift and the intensity effect have also been reported by Inamura and coworkers.¹⁶

IV. CONCLUSIONS

In conclusion, the comparison between experiment and simulation allows us to affirm that the BP in v-SiO₂ corresponds to the low-energy tail of a flattened transverse branch, whose center lies at relatively high energies. This is also in agreement with earlier studies,^{1,31} which ascribed these vibrations to hindered librations of coupled SiO₄ tetrahedra. The effect responsible for the occurrence of the BP which we have described here is valid for v-SiO₂, and it cannot be excluded that other mechanisms are active for different systems, like the idealized ones studied in Ref. 10. Nevertheless, it suggests a general approach for the study of the BP in glasses. It is well known that every kind of disorder induces a sort of level repelling and a consequent piling up of modes at the extremes of the vibrational spectrum, as shown by Elliott and coworkers, (see for instance Ref. 32 and references therein).

V. ACKNOWLEDGMENTS

We are grateful to Giancarlo Ruocco, Uli Buchenau and Stephen Elliott for very helpful discussions. This work was financially supported by INFN by PRA-GENFDT, Italian Ministero degli Affari Esteri, and MURST Progetto di Ricerca di Interesse Nazionale.

-
- ¹ U. Buchenau, M. Prager, N. Nücker, A. J. Dianoux, N. Ahmad and W. A. Philips, Phys. Rev. B **34**, 5665 (1986).
 - ² A. Fontana and G. Viliani, Phil. Mag. B **82**, (special issue) (2002).
 - ³ M. Foret, E. Courtens, R. Vacher and J. B. Suck, Phys. Rev. Lett. **77**, 3831 (1996).
 - ⁴ P. Benassi, M. Krisch, M. Masciovecchio, V. Mazzacurati, G. Monaco, G. Ruocco, F. Sette and R. Verbeni, Phys. Rev. Lett. **77**, 3835 (1996).
 - ⁵ R. Dell'Anna, G. Ruocco, M. Sampoli and G. Viliani, Phys. Rev. Lett. **80**, 1236 (1998).
 - ⁶ O. Pilla, A. Cunsolo, A. Fontana, C. Masciovecchio, G. Monaco, M. Montagna, G. Ruocco, T. Scopigno and F. Sette, Phys. Rev. Lett. **85**, 2136 (2000).
 - ⁷ J. L. Feldman, P. B. Allen and S. R. Bickham, Phys. Rev. B **59**, 3551 (1999).
 - ⁸ S. N. Taraskin, Y. L. Loh, G. Natarajan and S. R. Elliott, Phys. Rev. Lett. **86**, 1255 (2001).
 - ⁹ S. N. Taraskin, J. J. Ludlam, G. Natarajan and S. R. Elliott, Phil. Mag. B **82**, 197 (2002).
 - ¹⁰ T. S. Grigera, V. Martín-Mayor, G. Parisi and P. Verrocchio, Phys. Rev. Lett. **87**, 085502 (2001).
 - ¹¹ W. Götze and M. R. Mayr, Phys. Rev. E **61**, 587 (2000).
 - ¹² T. Theenhaus, R. Schilling, A. Latz and M. Letz, cond-mat/0105393 (2001).
 - ¹³ S. Sugai and A. Onera, Phys. Rev. Lett. **20**, 4210 (1966).
 - ¹⁴ C. S. Zha, R. J. Hemley, H. K. Mao, T. S. Duffy and C. Meade, Phys. Rev. B **50**, 13105 (1994).
 - ¹⁵ Y. Inamura, M. Arai, O. Yamamuro, A. Inaba, N. Kitamura, T. Otomo, T. Matsuo, S. M. Bennington and A. C. Hanon, Physica B **263/264**, 299 (1999).
 - ¹⁶ Y. Inamura, M. Arai, T. Otomo, N. Kitamura and U. Buchenau, Physica B **284-288**, 1157 (2000).
 - ¹⁷ D. J. Lacks, Phys. Rev. Lett. **84**, 4629 (2000).
 - ¹⁸ P. Jund and R. Jullien, J. Chem. Phys. **113**, 2768 (2000).
 - ¹⁹ O. Pilla, L. Angelani, A. Fontana, J. R. Gonçalves and G. Ruocco, J. Phys.: Condens. Matter **15**, S995 (2003).
 - ²⁰ M. Foret, R. Vacher, E. Courtens and G. Monaco, Phys. Rev. B **66**, 024204 (2002).
 - ²¹ E. Courtens, M. Foret, B. Helen, B. Rufflé and R. Vacher, Phys. Rev. B **66**, 024204 (2002).
 - ²² B. Rufflé, M. Foret, E. Courtens, R. Vacher and G.

- Monaco, J. Phys. Condens. Matter **15**, 1281 (2003).
- ²³ B. W. H. van Beest, G. J. Kramer and R. A. van Santen, Phys. Rev. Lett. **64**, 1955 (1990).
- ²⁴ Y. Guissani and B. Guillot, J. Chem. Phys. **104**, 7633 (1996).
- ²⁵ O. Pilla, S. Caponi, A. Fontana, M. Montagna, F. Rossi, G. Vilianni, L. Angelani, G. Ruocco, G. Monaco and F. Sette, cond-mat/0209519 (2003).
- ²⁶ S. N. Taraskin and S. R. Elliott, Phil. Mag. B **2**, 403 (1998).
- ²⁷ A. J. Leadbetter, J. Chem. Phys. **51**, 779 (1969).
- ²⁸ G. Carini, G. D'Angelo, G. Tripodo, A. Fontana, A. Leonardi, G. A. Saunders and A. Brodin, Phys. Rev. B **52**, 9342 (1995-I).
- ²⁹ A. Fontana, F. Rossi, G. Carini, G. D'Angelo, G. Tripodo and A. Bartolotta, Phys. Rev. Lett. **78**, 1078 (1997).
- ³⁰ C. A. Angell, Y. Yue and L-M. Wang, J. R. D. Copley, S. Borik and S. Mossa, J. Phys.: Condens. Matter **15**, S1051 (2003).
- ³¹ S. N. Taraskin and S. R. Elliott, Phys. Rev. B **56**, 8605 (1997).
- ³² S. I. Simdyankin, S. N. Taraskin, M. Elenius, S. R. Elliott and M. Dzugutov, Phys. Rev. B **65**, 104302 (2002).